Polarization Technology Meeting
October 14, 2025
https://indico.bnl.gov/event/30193/

Comments

A.A. Poblaguev

Brookhaven National Laboratory

BROOKHAVEN NATIONAL LABORATORY

Asymmetry and polarization

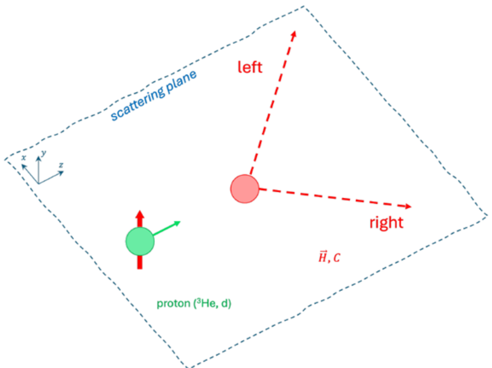

- Spin-dependent cross section

$$\sigma = \sigma_0(1 + A_y P_y \cos\phi) \qquad (1)$$

  - Unpolarized cross section σ_0
  - P_y vertical component of beam polarization $\vec{P} = (P_x, P_y, P_z)$
  - Analyzing power $A_y = \frac{1}{P_y}\frac{\sigma^{\text{left}} - \sigma^{\text{right}}}{\sigma^{\text{left}} + \sigma^{\text{right}}}$
  - Azimuth of scattered particle ϕ

Coulomb-nuclear interference (CNI) (see slide 37).)

- A_y: measure of polarization sensitivity of scattering process
- **At AGS and RHIC energies, no scattering processes available with A_y known to sufficient accuracy for** $\Delta P/P \leq 0.01$ [1].
- **Interference of EM and strong interaction at small scattering angles provides sizable analyzing power for elastic pp (and pN) scattering.**

Hadron Polarimetry at the Electron-Ion Collider   Vera Shmakova (vshmakova@bnl.gov)   6/32

Since *left* and *right* refer to the recoil particle direction, the definition should be

$$A_y = \frac{1}{P_y}\frac{\sigma^{\text{right}} - \sigma^{\text{left}}}{\sigma^{\text{right}} + \sigma^{\text{left}}}$$

(unless A_y defined with the opposite sign, i.e. $A_y = -A_N$).
The same correction applies to several other places throughout the presentation.

Transition frequencies between hyperfine states of H

Using Zeeman splitting (slide 14, Eq. (6)

- Determine transition frequencies f_{ij} between hyperfine states $|i\rangle$ and $|j\rangle$.
- Classification refers to change of quantum numbers (see Ramsey [5]):
  - B_0 is static field, B_1 is RF field that exerts torque on magnetic moment μ:
  - π ($B_1 \perp B_0$) transitions *within one* F multiplet:

$$\Delta F = 0, \quad \Delta m_F = \pm 1. \tag{9}$$

  - σ ($B_1 \parallel B_0$) transitions *between different* F multiplets:

$$\Delta F = \pm 1, \quad \Delta m_F = 0, \pm 1. \tag{10}$$

Eqs. (9) and (10) are incorrect.
Regardless of ΔF,

- $B_1 \perp B_0$ drives $\Delta m_F = \pm 1$ dipole magnetic transition
- $B_1 \parallel B_0$ drives $\Delta m_F = 0$

Hyperfine states of hydrogen

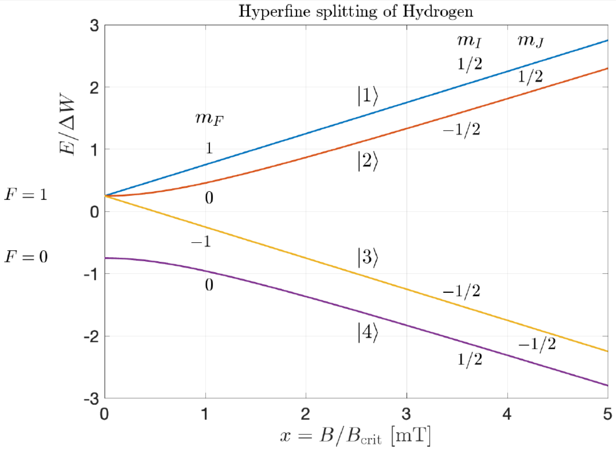

Critical field B_c (see slide 39)

- Zeeman energy $g_J \mu_B B$ comparable to $E_{\rm hfs}$
- $E_{\rm hfs} \approx 5.874 \times 10^{-6}$ eV (≈1420 MHz [3]):
- $B_c = 50.7$ mT

Transition frequencies

- Transition frequency between two hyperfine states $|i\rangle$ and $|j\rangle$ given by:

$$f_{ij} = \frac{E_{|i\rangle}(B) - E_{|j\rangle}(B)}{h} \qquad (6)$$

- **When f_{ij} matches one of the beam harmonics at a certain holding field $|\vec{B}|$, resonant depolarization occurs** [4]

	f_{ij}/f_b			$\exp(-f_{ij}^2/2\sigma_f^2)$
	124 mT	127 mT	130 mT	127 mT
f_{12}^{π}	6.293	6.327	6.359	7.73×10^{-1}
f_{34}^{π}	9.371	9.337	9.305	5.65×10^{-1}
f_{23}^{π}	32.029	32.922	33.817	8.79×10^{-4}
$f_{13}^{2\gamma}$	38.322	39.249	40.176	4.53×10^{-5}
f_{24}^{σ}	41.399	42.259	43.121	9.21×10^{-6}
f_{14}^{π}	47.692	48.586	49.480	2.21×10^{-7}

TABLE II. Transition frequencies (in units of f_b) for the EIC flattop. Parameters: $N_b = 1160$, $f_b = 90.683$ MHz, $\sigma_t = 0.2$ ns.

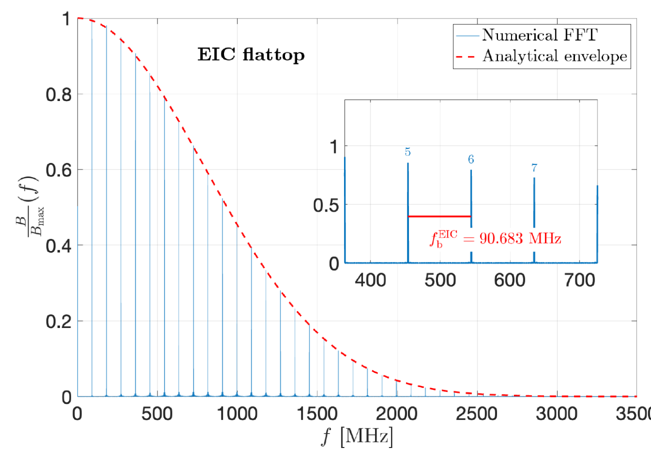

This is not always true. On resonance the transition probability is $w_{ij} = \sin^2(\pi f_R t)$.

Since $f_R \propto (I_{\rm beam}/\sigma_r) \times \exp(-f_{ij}^2/2\sigma_f^2)$ $[\sigma_f = (2\pi\sigma_t)^{-1} = 0.8\ {\rm GHz}]$ the Rabi frequency f_R — and hence w_{ij} —becomes extremely small for large $f_{ij} \gtrsim 3$ GHz.

For example, with $B_h = 127$ mT, $\sigma_t = 0.2$ ns, and $t_{\rm int} \sim 30$ µs one finds $w_{23} \sim 2 \cdot 10^{-4}$ and $w_{13}, w_{24}, w_{14} \ll 10^{-4}$ even if f_{ij} **exactly matches** a beam harmonic.

Elimination of beam-induced H target depolarization at EIC

Solutions

1. At RHIC, B-field was moved to $\approx 120\,\mathrm{mT}$ and $\frac{f_{ij}}{f_b^{\mathrm{RHIC}}} \geq 350$ ignored (slide 19)
2. **For EIC:** $\Rightarrow$ **push harmonics to** $\geq 100 \Rightarrow$ **holding field** $\geq 400\,\mathrm{mT}$

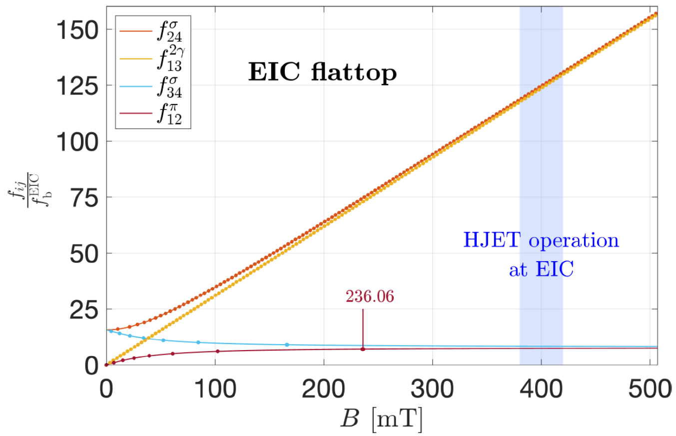

Resonances f_{34}^{σ} and f_{12}^{π}

- Become harmless (die out) above $\approx 236.6\,\mathrm{mT}$

- Potentially strong resonances f_{12} and f_{34} can be easily and reliably avoided by keeping the holding field within $120 < B_h < 140$ mT.
- For $B_h = 127$ mT, the combined depolarization due to these resonances,

$$w_{ij} = \frac{\left(f_R^{ij}\right)^2}{\left(f_{harm} - f_{ij}\right)^2 + \left(f_R^{ij}\right)^2} \sin^2\left(\pi\sqrt{\left(f_{harm} - f_{ij}\right)^2 + \left(f_R^{ij}\right)^2}\, t\right)$$

was evaluated (by solving quantum-mechanical equations) to be aspproximately **0.06%**

Conclusions: Critical technical developments

Solved challenges

1. EIC's tenfold increase in bunch frequency creates **electromagnetic harmonics resonantly drives hyperfine transitions** in hydrogen atoms at RHIC's HJET holding field of 120 mT. Operating at 400 mT shifts transitions safely above populated harmonics and restores robust target polarization (see [2]).
2. **pC target heating under control:** Larger beam sizes at the pC location reduce areal power density; thermal modeling keeps T_{max} below carbon sublimation. Risk #128 downgraded.
3. **pC wakefield mitigation:** CST studies show **dielectric holders** (e.g. Al_2O_3) with a thin 10 nm Au coating (charge control) significantly lower wake impedance vs. metallic designs.

Key decisions / principles

1. Baseline **HJET holding field:** 400 mT (vector-capable when feasible; B_y-only acceptable initially if the chamber preserves an upgrade path).
2. Prefer **dielectric pC holders**, RF hygiene near ports/feedthroughs, and one-target-in-chamber operation to minimize impedance.
3. Co-located polarimetry at **IP4** to minimize spin-transport systematics among pC/HJET/^{3}He.

- Increasing the holding field does not help to suppress beam-induced depolarization and may, in fact, significantly increase systematic uncertainties in polarization measurements.
- There is no need to raise the holding field if $\sigma_t \geq 0.2$ ns.

Outlook: Ongoing developments

Ongoing developments

1. **HJET holding-field system:** engineer magnet + chamber; assess compensation for $\int B_{x,y,z}\, d\ell$; preserve vector B_x, B_y, B_z option.
2. **HJET detector system:** increased azimuthal coverage/segmentation to access (P_x, P_y, P_z); track recoils in measured guide-field maps.
3. **HJET H_2 systematics:** typical ABS H_2 at target 3 % to 4 % ⇒ integrate QMA into BRP to accurately determine H_2 fraction;
4. **Bunch-by-bunch polarimetry:** detector/readout able to resolve 11 ns spacing (fast Si or diamond; bunch-synchronous timing). Finalize before FDR.
5. **pC target thermal validation:** direct temperature measurements during beam (RHIC) and extension to IP6 conditions.
6. **pC vacuum transfer chamber:** enable target swaps without breaking ring vacuum; reduce contamination and downtime.
7. **^{3}He ABS:** cryogenic source at 1 K under development at MIT; align readiness with EIC early light-ion operations.

$$\phi_1(s,t) = \langle ++|M|++\rangle,$$
$$\phi_2(s,t) = \langle ++|M|--\rangle,$$
$$\phi_3(s,t) = \langle +-|M|+-\rangle,$$
$$\phi_4(s,t) = \langle +-|M|-+\rangle,$$
$$\phi_5(s,t) = \langle ++|M|+-\rangle.$$

$$\phi_+ = \tfrac{1}{2}(\phi_1 + \phi_3),$$
$$\phi_- = \tfrac{1}{2}(\phi_1 - \phi_3),$$

- In my estimates, P_z cannot be measured with sufficient accuracy by HJET unless the hadronic non-flip amplitude $\phi_-(t)$ is anomalously large $|\phi_-/\phi_+| \gg 10^{-3}$ at EIC beam energies.
- According to N.H.Buttimore *et al.*, Phys. Rev. D **59**, 114010 (1999) : "There is persuasive evidence both from experiment and from dynamical arguments that ϕ_- is exceedingly small at high energies: $|\phi_-/\phi_+| < 10^{-3}$ for energies beyond $p_L = 200$ GeV/c".

Outlook: Ongoing developments

Ongoing developments

1. **HJET holding-field system:** engineer magnet + chamber; assess compensation for $\int B_{x,y,z}\,d\ell$; preserve vector B_x, B_y, B_z option.
2. **HJET detector system:** increased azimuthal coverage/segmentation to access (P_x, P_y, P_z); track recoils in measured guide-field maps.
3. **HJET H_2 systematics:** typical ABS H_2 at target 3 % to 4 % ⇒ integrate QMA into BRP to accurately determine H_2 fraction;
4. **Bunch-by-bunch polarimetry:** detector/readout able to resolve 11 ns spacing (fast Si or diamond; bunch-synchronous timing). Finalize before FDR.
5. **pC target thermal validation:** direct temperature measurements during beam (RHIC) and extension to IP6 conditions.
6. **pC vacuum transfer chamber:** enable target swaps without breaking ring vacuum; reduce contamination and downtime.
7. **^{3}He ABS:** cryogenic source at 1 K under development at MIT; align readiness with EIC early light-ion operations.

- What accuracy in determining the fraction of H_2 fraction (originating from the nozzle) can be achieved with the QMA?
- Even if a precision well below 1% were technically possible, the QMA alone cannot provide an accurate evaluation of the background, since it cannot account for the following effects:
  - ✓ Atomic hydrogen and/or protons present in the beam gas,
  - ✓ Partial polarization of the recombined H_2,
  - ✓ Background arising from beam proton scattering on nuclei in the jet, beam gas, or surrounding walls.
- Therefore, the QMA should be regarded only as an **auxiliary diagnostic** to support the background evaluation method developed for RHIC HJET.

The polarized H and D atomic beam source for ANKE at COSY-Jülich

Nuclear Instruments and Methods in Physics Research A 721 (2013) 83–98

Fig. 24. Spatial distributions of $H_1(\bullet), H_2(\circ)$ and degree of dissociation ($\blacksquare$) averaged over 3 mm wide bands in the *xz* and *yz* planes, respectively (here the *z*-axis is the geometrical axis of the ABS).

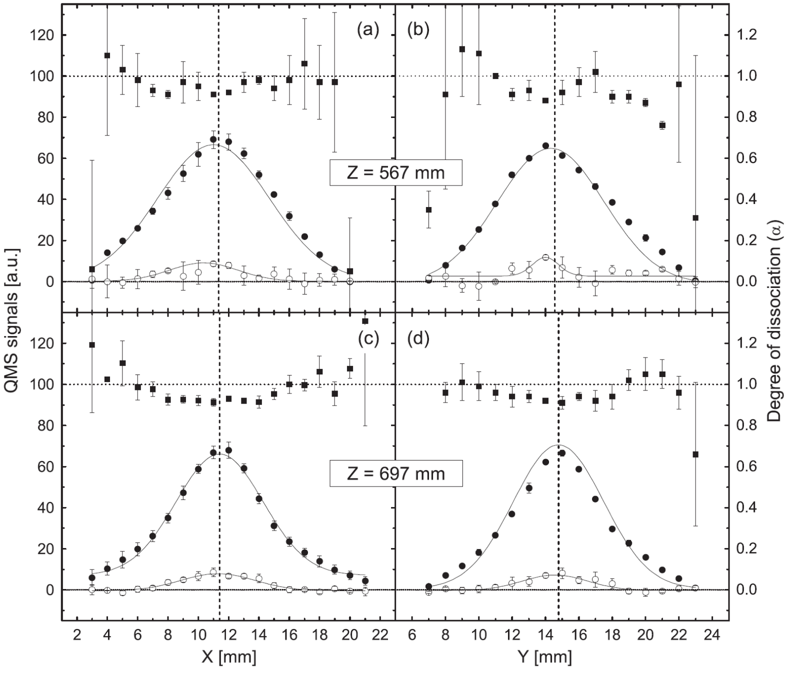

The admixture of molecules in an atomic beam is described by the degree of dissociation

$$\alpha = \frac{\rho_a}{\rho_a + 2 \cdot \rho_m} \quad (4)$$

6.1. Measurements with crossed-beam QMS

The measured profiles of the atomic fraction (identical to those of Fig. 21), those of the molecular fraction, and those of the degree of dissociation, deduced from Eq. (6), are collected in Fig. 24. As it is seen from the figure, the distribution of the degree of dissociation shows a dip around the central line due to the higher density of molecular hydrogen originating from the nozzle. The mean value in an aperture of 10 mm diameter results as $\overline{\alpha} = 0.95 \pm 0.04$.

- After accounting for systematic errors, no evidence remains that molecular hydrogen originating from the nozzle contributes significantly (or noticeably) to the jet beam.
- In QMS measurements, however, the systematic uncertainty in evaluating the H_2 fraction is unacceptably large for EIC requirements.
- Notably, It had been observed that the nuclear polarization in recombined hydrogen is partially retained after recombination.

Backup

Polarized ^{3}He Atomic Beam Source

Original MIT development for nEDM exp't at Oakridge

- Prajwal T. MohanMurthy, J. Kelsey, J. Dodge, R. Redwine, R. Milner, P. Binns, B. O'Rourke
- nEDM experiment at ORNL discontinued

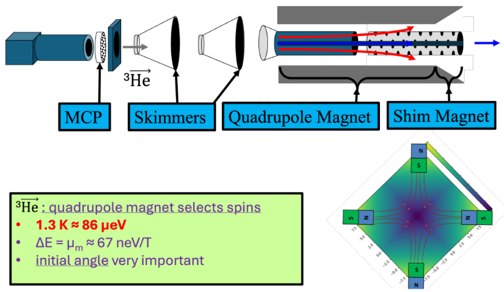

Atomic flux

- With $1 \times 10^{14}\,\mathrm{s}^{-1} \Rightarrow$ bare-jet $d_t \approx 1.3 \times 10^{10}\,\mathrm{cm}^{-2}$
  - Assumptions: $D = 1.0$ cm (uniform), $L = 1$ cm, $T = 1.3$ K.
- With storage cell (molecular flow, $T = 77$ K): $d_t \approx 1.0 \times 10^{12}\,\mathrm{cm}^{-2}$
  - Geometry: $\ell_{inj} = 10$ cm, $\ell_{up} = \ell_{down} = 30$ cm, $\ell_t = 60$ cm (see slide 64).
- **Well-suited for absolute $^3\vec{He}^{++}$ beam polarimetry at EIC.**

Hadron Polarimetry at the Electron-Ion Collider   Vera Shmakova (vshmakova@bnl.gov)   28/32

When designing a polarized ^{3}He atomic beam source for the EIC, it should be kept in mind that the systematic uncertainties in the ^{3}He beam polarization measurements may differ significantly from those in HJET.

- The kinematic distributions of recoil particles in the ^{3}He recoil spectrometer differ substantially from those in HJET.
- Breakup of the target ^{3}He nuclei may strongly distort the measured time–amplitude distribution.